

# Bohmian Mechanics, the Quantum-Classical Correspondence and the Classical Limit: The Case of the Square Billiard

A. Matzkin

Received: 20 June 2008 / Accepted: 22 January 2009 / Published online: 7 April 2009  
© Springer Science+Business Media, LLC 2009

**Abstract** Square billiards are quantum systems complying with the dynamical quantum-classical correspondence. Hence an initially localized wavefunction launched along a classical periodic orbit evolves along that orbit, the spreading of the *quantum* amplitude being controlled by the spread of the corresponding *classical* statistical distribution. We investigate wavepacket dynamics and compute the corresponding de Broglie-Bohm trajectories in the quantum square billiard. We also determine the trajectories and statistical distribution dynamics for the equivalent classical billiard. Individual Bohmian trajectories follow the streamlines of the probability flow and are generically non-classical. This can also hold even for short times, when the wavepacket is still localized along a classical trajectory. This generic feature of Bohmian trajectories is expected to hold in the classical limit. We further argue that in this context decoherence cannot constitute a viable solution in order to recover classicality.

**Keywords** Quantum-classical correspondence · Bohmian mechanics · Classical limit · Square billiard

## 1 Introduction

The de Broglie-Bohm (BB) theory of motion is generally regarded as the main alternative to standard quantum mechanics (QM). The main achievement of the theory in the non-relativistic domain is to deliver an interpretative framework accounting for quantum phenomena in terms of point-like particles guided by objectively existing waves along deterministic individual trajectories [1]. Although the formalism does

---

A. Matzkin (✉)

Laboratoire de Spectrométrie Physique (CNRS Unité 5588), Université Joseph-Fourier Grenoble-1,  
BP 87, 38402 Saint-Martin d'Hères, France  
e-mail: alexandre.matzkin@ujf-grenoble.fr

not give predictions going beyond those of QM, it is often argued that BB should be favored because of its interpretational advantages stemming from the ontological continuity between the classical and the quantum domains. Thus, the so-called ‘Bohmian’ trajectories followed by the quantum particle should be regarded as objectively real as the trajectories of classical mechanics [2], without the need to make a cut between the descriptions of reality at the classical and the quantum levels [3, 4].

The aim of the present work is to investigate Bohmian trajectories in square billiards and contrast them with the trajectories of the corresponding classical system. A square billiard is the two-dimensional version of the particle in a box problem, which was the example employed by Einstein in his criticism of Bohm’s rediscovery of de Broglie’s pilot-wave [5]. The interest of square billiards is that in terms of the quantum-classical dynamical correspondence, the quantum mechanical propagator is constructed from classical trajectories. Hence the quantum dynamics of a time-dependent wavefunction is readily understood from the underlying classical dynamics—each point of the wavefunction follows a classical trajectory. On the other hand Bohmian trajectories are generically markedly different from their classical counterpart: the Bohmian trajectories propagate by following the probability flow, which results from the interference of several bits of the wavefunction, each of which propagates by following a classical trajectory. There is no criterion or limiting process (involving high energies, macroscopic size, etc.) that will make the Bohmian trajectories resemble or tend toward those of the classical billiard for a closed system.

Thus, although having BB trajectories irremediably different from the classical ones in a closed system may not be a problem in itself, we will argue that when a quantum system displays the fingerprints of classical motion, this creates difficulties in view of the advantages traditionally attributed to the BB interpretation. We will further contend that the way that is generally favoured [6] in achieving the classical limit from Bohmian trajectories, based on the decoherence resulting from the interaction of the system with its environment, suffers from a lack of consistency: we will question, in view of the quantum-classical correspondence, whether requiring localized and non-spreading wavefunctions is the correct way to define the classical limit for the BB interpretation.

We will proceed as follows. We will first give in Sect. 2 a brief account of the classical square billiard, introducing the trajectories and the propagation of classical statistical ensembles. Section 3 will deal with the quantum square billiard, focusing on the propagation of initially localized wavepackets. We will then (Sect. 4) give a brief overview of the de Broglie-Bohm theory and display the Bohmian trajectories for the wavepackets previously shown in Sect. 3. The results as well as their implications regarding the classical limit will be discussed in Sect. 5 and a summary with our conclusions will be exposed in Sect. 6.

## 2 The Classical Square Billiard

### 2.1 Classical Trajectories and Periodic Orbits

A square billiard is a two dimensional box in the  $(x, y)$  plane containing a particle, which moves freely except for the specular bounces produced when it hits one of the

walls. Let  $E = (p_x^2 + p_y^2)/2m$  be the total energy of the particle and  $L$  the length of one side of the square. Let  $(x_0, y_0)$  denote the initial position of the particle. The classical trajectory followed by the particle is readily obtained by integrating the equations of motion (it is convenient to unfold the square box by propagating the trajectory in free motion beyond the wall and then fold back the trajectory to the original square [7]). There are two types of orbits: either the particle retraces the trajectory—one obtains a periodic orbit (PO)—, or else the trajectory covers entirely the billiard. Since the momentum is conserved, the condition for a PO is that the trajectory appears closed in the  $(x, y)$  plane, which is possible if

$$\frac{p_x}{p_y} = \frac{n_y}{n_x} \tag{1}$$

where  $n_x$  and  $n_y$  count the number of bounces off the  $x$  and  $y$  axes respectively, and are therefore integers. A non periodic trajectory will be obtained if  $p_x/p_y$  is irrational.

Note that the PO condition only depends on the momenta: if a particle is launched with the same momenta from two nearby initial positions, the two periodic orbits will evolve in the same way, the PO's being deformed one relative to the other, as in the example shown in Fig. 1(a). On the other hand if the second initial conditions also involve a change in the momenta, the ensuing trajectory will not be periodic and will deviate in time from the PO, as portrayed in Fig. 1(b). The period  $T_{PO}$  of a periodic orbit is given by

$$T_{PO} = L \frac{\sqrt{n_x^2 + n_y^2}}{\sqrt{p_x^2 + p_y^2}} \tag{2}$$

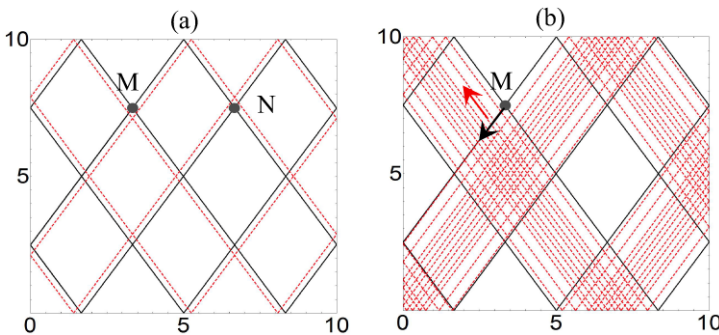


**Fig. 1** Classical trajectories in a square billiard with sides of length  $L = 10$  (arbitrary units). **(a)** A classical periodic orbit (PO), going through the points labeled  $M$  and  $N$  is shown in black. The grey dashed (online: red) line shows a trajectory launched near  $M$  with the same momenta as the black PO; it is also a PO. **(b)** Two trajectories are launched from  $M$ : the first one in black is the PO shown in **(a)**. The second, in dashed grey (online: red) has slightly different initial momenta, which is enough to render the trajectory non-periodic (the red arrow shows the position of the trajectory slightly after  $t \sim 5T_{PO}$ )

### 2.2 Classical Distributions Dynamics

The most general classical distribution  $\rho(\mathbf{x}, \mathbf{p}, t)$  should be considered in phase space.  $\rho$  gives a density of particles having positions  $\mathbf{x} = (x, y)$  and momenta  $\mathbf{p} = (p_x, p_y)$ . The time evolution of  $\rho$  from an initial density  $\rho_0(\mathbf{x}, \mathbf{p})$  is governed by Liouville’s theorem

$$\frac{\partial \rho}{\partial t} = \{H, \rho\}, \tag{3}$$

a statement of the conservation of the flow in phase-space,  $d\rho/dt = 0$ ;  $\{, \}$  denotes the Poisson bracket. Inside the billiard the Hamiltonian  $H = \mathbf{p}^2/2m$  is trivial. The bounces due to the wall can be treated as above by considering first free motion for the distribution and then appropriately folding it back inside the square. In terms of the configuration space variables, (3) takes the form

$$\frac{\partial \varrho}{\partial t} + \frac{1}{m} \nabla_{\mathbf{x}} \int \rho(\mathbf{x}, \mathbf{p}, t) \mathbf{p} d\mathbf{p} = 0 \tag{4}$$

where

$$\varrho(\mathbf{x}, t) \equiv \int \rho(\mathbf{x}, \mathbf{p}, t) d\mathbf{p} \tag{5}$$

is the configuration space density. Note that if the momentum is a pre-assigned function of a position dependent momentum field  $\mathbf{P}(\mathbf{x}, t)$ , the phase-space density takes the form  $\rho(\mathbf{x}, \mathbf{p}, t) = \varrho(\mathbf{x}, t) \delta(\mathbf{p} - \mathbf{P}(\mathbf{x}, t))$  and (4) becomes

$$\frac{\partial \varrho}{\partial t} + \frac{1}{m} \nabla_{\mathbf{x}} (\varrho(\mathbf{x}, t) \mathbf{P}(\mathbf{x}, t)) = 0. \tag{6}$$

In classical mechanics, the field in configuration space is well-known to be given [8] in terms of the classical action  $\mathcal{S}(\mathbf{x}_0, \mathbf{x}, t)$  via

$$\mathbf{P}(\mathbf{x}, t) \equiv \nabla_{\mathbf{x}} \mathcal{S}(\mathbf{x}_0, \mathbf{x}, t), \tag{7}$$

ensuring that the mechanical momentum is recovered. Note that  $\mathbf{P}$  and  $\mathcal{S}$  are in general multivalued fields.

Classically, any normalized distribution can be envisaged. We will work with initial distributions fairly well localized in configuration space. If each point of the distribution has the same initial momentum obeying (1), the propagation of the ensemble is straightforward—the ensemble moves along the family of neighboring periodic orbits as in Fig. 1(a). However, anticipating on the analogy with the quantum mechanical square billiard, we will choose initial distributions admitting a dispersion in the momenta; the ensemble will then spread as it propagates. To be specific, let

$$\begin{aligned} \rho_0(\mathbf{x}, \mathbf{p}) = \pi^{-2} \exp \left[ -\frac{(x - x_0)^2}{2d^2} - 2\Delta^2 (p_x - p_{x_0})^2 \right] \\ \times \exp \left[ -\frac{(y - y_0)^2}{2d^2} - 2\Delta^2 (p_y - p_{y_0})^2 \right] \end{aligned} \tag{8}$$

where  $d$  and  $\Delta$  are parameters that control the widths of the Gaussians. By integrating over the momenta, we obtain

$$\varrho_0(\mathbf{x}) = \frac{\exp[-\frac{(x-x_0)^2}{2d^2}] \exp[-\frac{(y-y_0)^2}{2d^2}]}{2\pi d^2}. \tag{9}$$

The usual properties of Gaussian distributions,

$$\langle x \rangle = x_0 \quad \langle x^2 \rangle = x_0^2 + d^2, \tag{10}$$

$$\langle p_x \rangle = p_{x_0} \quad \langle p_x^2 \rangle = p_{x_0}^2 + 1/4\Delta^2 \tag{11}$$

are verified (as well as the same properties for  $y$ ). A solution of the Liouville equation  $\rho(\mathbf{x}, \mathbf{p}, t)$  follows by replacing  $\mathbf{x} \rightarrow \mathbf{x} - \mathbf{p}t/m$  in (8); integrating over the momenta yields

$$\varrho(\mathbf{x}, t) = \frac{\exp[-\frac{2m^2\Delta^2}{t^2+4d^2m^2\Delta^2}((x_0-x+\frac{p_{x_0}t}{m})^2+(y_0-y+\frac{p_{y_0}t}{m})^2)]}{\frac{\pi t^2}{2\Delta^2m^2}+2\pi d^2}. \tag{12}$$

Hence in configuration space, the initially localized classical distribution spreads in time, the spreading being controlled by the width of the initial Gaussian  $d$ . We will further employ in this work only distributions characterized by  $\Delta = d$  (holding for the chosen units), so that the product of the variances  $V(x)V(p_x)$ , readily obtained from (10) and (11) does not depend on  $d$  or  $\Delta$ .

An example is illustrated in Fig. 2: a distribution of the form (8) is initially placed at  $\mathbf{x}_0 \equiv \mathbf{x}_M$  lying on the periodic orbit shown in Fig. 1(a) with  $\mathbf{p}_0 \equiv \mathbf{p}_M$  in the direction of the arrow along the PO. Figure 2 shows snapshots taken at different times, as the distribution spreads and becomes nearly uniform for  $t \sim 100T_{PO}$ . Note that due to the linearity of the Liouville equation, one can classically envisage to take as the initial distribution the sum of two Gaussians (9) localized at two different points of the billiard. The evolution for the ensemble is then obtained by linear superposition of the evolution of the two Gaussians, as illustrated in Fig. 3 for a distribution obtained by superposing two ensembles initially localized on two points of the periodic orbits  $\mathbf{x}_M$  and  $\mathbf{x}_N$ .

### 3 The Quantum Square Billiard

#### 3.1 Eigenstates and Propagator

The eigenstates in configuration space and eigenvalues of the quantum billiard are readily obtained from those of the infinite well problem,

$$\psi_{n_x, n_y}(x, y) = \frac{2}{L} \sin \frac{n_x \pi x}{L} \sin \frac{n_y \pi y}{L}, \tag{13}$$

$$E(n_x, n_y) = \frac{\hbar^2 \pi^2}{2mL^2} (n_x^2 + n_y^2). \tag{14}$$

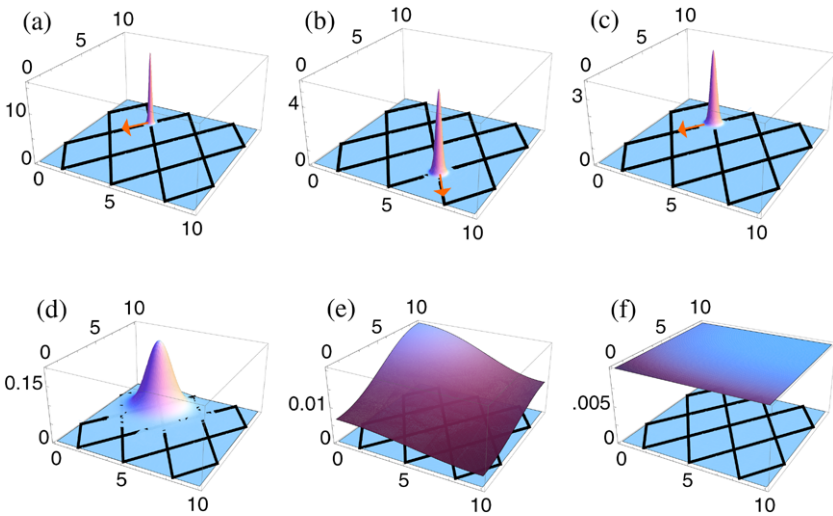


**Fig. 2** Time evolution of a *classical distribution* in configuration space. (a) At  $t = 0$  the classical distribution given by (8) is a Gaussian centered on  $M$ , with  $\mathbf{p}_M$  in the direction of the arrow, along the periodic orbit shown in Fig. 1 (plotted in black). The height of the normalized distribution is given in arbitrary units that are nevertheless the same in all the figures. The centre of the distribution follows the periodic orbit. (b) gives a snapshot at  $t = 3/4 T_{PO}$  and (c) at  $t = T_{PO}$  (first return at  $M$ ). The initial classical distribution spreads with increasing time; (d) shows the distribution at  $t = 5 T_{PO}$ . For longer times, the distribution in the box becomes a folded Gaussian: (e) shows the distribution at  $t = 25 T_{PO}$  and (f) at  $t = 100 T_{PO}$ , when the distribution is nearly uniform

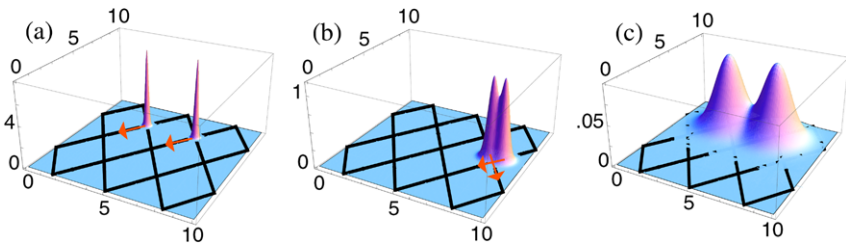


**Fig. 3** Time evolution of a *classical distribution* composed of two initially localized Gaussian components. (a) At  $t = 0$  the classical distribution is given by two equal Gaussians centered at  $M$  and  $N$ , with  $\mathbf{p}_M$  and  $\mathbf{p}_N$  in the direction of the arrows, along the same periodic orbit shown in Fig. 1. Each Gaussian follows the periodic orbit, spreading as the time evolves. The two Gaussians must cross at several points before returning to their respective initial points. (b) shows the distribution slightly before the two Gaussians superpose when they cross at  $t = (11/8) T_{PO}$ . (c) shows the situation at  $t = 5 T_{PO}$ . The initial Gaussians have sufficiently spread so that their wings superpose. At longer times, one obtains the type of behaviour shown in Fig. 2(f)

The propagator—the configuration space representation of the time evolution operator—is that of the free particle with an appropriate folding into the original square. The free particle propagator takes the well known form

$$K(\mathbf{x}_0, \mathbf{x}, t) = \frac{m}{2\pi\hbar t} \exp\left(\frac{im}{2\hbar t} [(x_0 - x)^2 + (y_0 - y)^2] - i\frac{\pi}{2}\right), \quad (15)$$

which in the square billiard is exact for short times (no bounces on the walls). We will omit to give explicitly the additional terms accounting for the bounces that must be added to (15) (see e.g. Chap. 6 of [9] for the full expression). Instead it will be more convenient for interpretational purposes to employ the semiclassical form of  $K$ . Recall that for free or quadratic potentials, the semiclassical approximation to the propagator is exact: the semiclassical propagator is given by [10]

$$K(\mathbf{x}_0, \mathbf{x}, t) = \sum_k \frac{1}{2i\pi\hbar} \left| \det \frac{\partial^2 \mathcal{S}_k}{\partial \mathbf{x} \partial \mathbf{x}_0} \right|^{1/2} \exp(i\mathcal{S}_k(\mathbf{x}_0, \mathbf{x}, t)/\hbar + i\phi_k), \tag{16}$$

where the sum runs on all the classical trajectories  $k$  connecting  $\mathbf{x}_0$  to  $\mathbf{x}$  in the time  $t$ .  $\mathcal{S}_k$  is the classical action for the  $k$ th trajectory and the determinant is the inverse of the Jacobi field familiar from the classical calculus of variations, reflecting the local density of the paths.  $\phi_k$  is a phase that takes into account the bounces on the hard wall.

### 3.2 Quantum Dynamics

We will take for the initial wavefunction the localized Gaussian

$$\psi_0(\mathbf{x}) = \frac{1}{d\sqrt{2\pi}} \exp \frac{-(x - x_0)^2 - (y - y_0)^2}{4d^2} \exp \frac{i}{\hbar}(xp_{x_0} + yp_{y_0}). \tag{17}$$

$p_{x_0}$  and  $p_{y_0}$  can be taken as parameters, though their physical meaning is revealed by taking the Fourier transform or computing the averages

$$\langle \hat{X} \rangle_{\psi_0} = x_0 \quad \langle \hat{X}^2 \rangle_{\psi_0} = x_0^2 + d^2, \tag{18}$$

$$\langle \hat{P}_x \rangle_{\psi_0} = p_{x_0} \quad \langle \hat{P}_x^2 \rangle_{\psi_0} = p_{x_0}^2 + \hbar^2/4d^2, \tag{19}$$

which unsurprisingly are the same as the classical ones if one puts  $\Delta \sim d/\hbar$ .

The time evolved wavefunction,

$$\psi(\mathbf{x}, t) = \int d\mathbf{x}' K(\mathbf{x}', \mathbf{x}, t) \psi_0(\mathbf{x}') \tag{20}$$

is readily computed by employing (15), giving the probability density

$$|\psi_{ST}(\mathbf{x}, t)|^2 = \frac{\exp[-\frac{2m^2}{\hbar^2 t^2/d^2 + 4d^2 m^2} ((x_0 - x + \frac{p_{x_0} t}{m})^2 + (y_0 - y + \frac{p_{y_0} t}{m})^2)]}{\frac{\pi \hbar^2 t^2}{2d^2 m^2} + 2\pi d^2}. \tag{21}$$

This expression is exact for the free particle, but is only valid for *very short times* in the square billiard. Note nevertheless that the probability density propagates exactly like the classical distribution (12). The additional terms due to the bounces that need to be added to (16) can produce interferences at longer times, as is apparent by using the expression (16) of the propagator. Indeed, if there are several points  $\mathbf{x}'$  such that  $\psi_0(\mathbf{x}')$  is non-vanishing that are propagated to the same  $\mathbf{x}$  in the time  $t$ , different trajectories will contribute to  $K$  in (20), leading to interferences. This means that

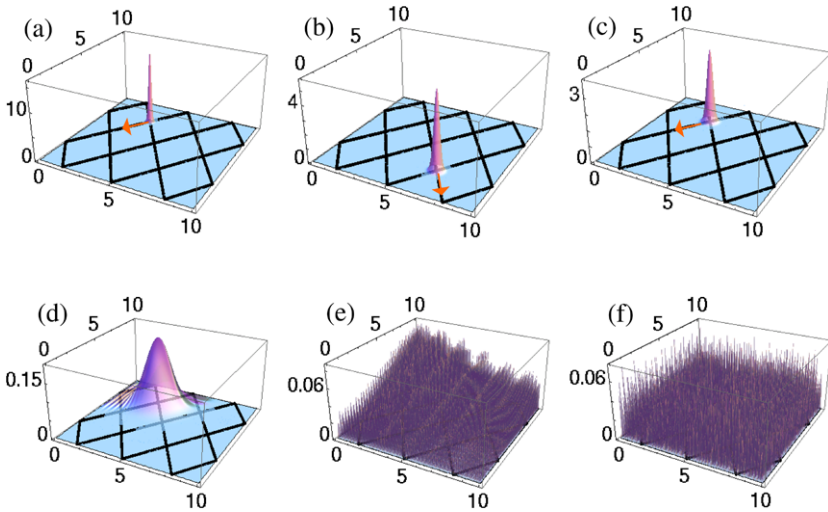


**Fig. 4** Time evolution of the *quantum probability density* in configuration space. (a) At  $t = 0$  the initial wavefunction is given by (17) with  $\mathbf{x}_0 \equiv \mathbf{x}_M$  and  $\mathbf{p}_0 \equiv \mathbf{p}_M$ . The parameters are chosen to match exactly those of the classical distribution illustrated in Fig. 2 (hence we take  $\hbar = 1$ ). With these parameters, the wavefunction leaves the region around  $M$  in the direction of the arrow and propagates along the classical periodic orbit. (b), (c) and (d) give snapshots of  $|\psi|^2$  at  $t = 3/4T_{PO}$ ,  $t = T_{PO}$ , and  $t = 5T_{PO}$  respectively. The evolution and spreading of the quantum probability density is nearly identical to that of the classical counterpart in Fig. 2. (e) and (f) shows the quantum probability distribution at  $t = 25T_{PO}$  and  $t = 100T_{PO}$  respectively. For longer times, interference resulting from the reflection of the distribution as it spreads creates a very high density of peaks, though as in the other cases, the smoothed quantum distribution corresponds to the classical one

each point  $\mathbf{x}'$  of the initial wavefunction is carried by a classical trajectory to the final point  $\mathbf{x}$ , interferences happening when several classical trajectories each carrying a part of the propagating wavefunction arrive simultaneously at  $\mathbf{x}$ .

Summarizing, we can say that the quantum propagation of the initial wavefunction is exactly like the propagation of an analog classical distribution, except for the provision of the wavefunction superposition (whereas in the classical case the superposition concerns the positive valued distribution themselves). Examples are given in Figs. 4 and 5. In Fig. 4 the initial wavefunction is of the form (17) with  $\mathbf{x}_0 \equiv \mathbf{x}_M$  and  $\mathbf{p}_0 \equiv \mathbf{p}_M$  in perfect correspondence with the classical distribution lying on the periodic orbit shown in Fig. 2. Figure 5 combines in the initial wavefunction two Gaussians at  $\mathbf{x}_M$  and  $\mathbf{x}_N$  with respective parameters  $\mathbf{p}_M$  and  $\mathbf{p}_N$  matching those of the classical distribution pictured in Fig. 3. We take as the initial wavefunction

$$\psi(\mathbf{x}, t = 0) = \frac{1}{\sqrt{2}}(\psi_M(\mathbf{x}) - \psi_N(\mathbf{x})) \tag{22}$$

which is one choice among many other possibilities leading to an initial quantum density matrix whose diagonal elements in the position representation match the initial classical distribution of Fig. 3.

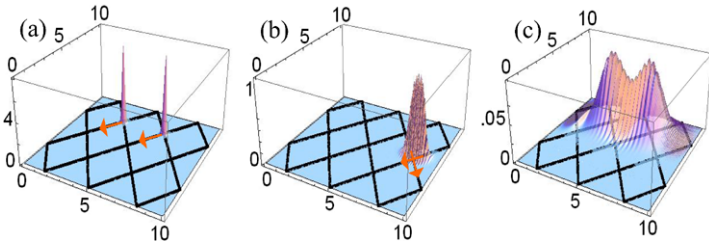


**Fig. 5** Time evolution of the *quantum probability density* in configuration space when the initial wavefunction is given by (22). (a) At  $t = 0$  the initial wavefunction is composed of two Gaussians centered respectively at  $M$  and  $N$ , each Gaussian leaving in the direction of the arrow along the classical periodic orbit. The diagonal position density matrix elements for this initial situation corresponds to the classical distribution portrayed in Fig. 3(a). (b) shows  $|\psi|^2$  slightly before the two Gaussians cross at  $t = (11/8)T_{PO}$  (compare with Fig. 3(b)). (c) shows the situation at  $t = 5T_{PO}$ ; the overlap of the two components of the spreading wavefunction results in interferences relative to Fig. 3(c)

### 4 Bohmian Mechanics of the Square Billiard

#### 4.1 General Remarks

The de Broglie-Bohm theory proposes to interpret quantum phenomena in terms of a point-like particle propagating along well-defined deterministic trajectories in configuration space through the guidance of the wavefunction (excellent accounts of the theory are given in Refs. [1, 6]). The initial position of the particle, and therefore its precise trajectory cannot be known, and this is why only statistical predictions can be made; these match the predictions of standard quantum mechanics. Employing the polar decomposition

$$\psi(\mathbf{x}, t) = R_{\psi}^{1/2}(\mathbf{x}, t) \exp(iS_{\psi}(\mathbf{x}, t)/\hbar), \tag{23}$$

the Schrödinger equation in terms of  $R$  and  $S$  yields the coupled equations

$$\frac{\partial R_{\psi}(\mathbf{x}, t)}{\partial t} + \frac{1}{m} \nabla \cdot (R_{\psi}(\mathbf{x}, t) \nabla S_{\psi}(\mathbf{x}, t)) = 0 \tag{24}$$

and

$$\frac{\partial S_{\psi}(\mathbf{x}, t)}{\partial t} + \frac{(\nabla S_{\psi}(\mathbf{x}, t))^2}{2m} + V(\mathbf{x}, t) + Q_{\psi}(\mathbf{x}, t) = 0, \tag{25}$$

where  $V(\mathbf{x}, t)$  is the usual potential (that vanishes here except on the billiard’s boundaries) and  $Q_{\psi}(\mathbf{x}, t)$  is a term known as the quantum potential given by

$$Q_{\psi}(\mathbf{x}, t) \equiv -\frac{\hbar^2}{2m} \frac{\nabla^2 R_{\psi}^{1/2}}{R_{\psi}^{1/2}}. \tag{26}$$

The momentum and the velocity of the particle are introduced via a configuration space field defined from the polar phase function through

$$\mathbf{p}_{\psi}(\mathbf{x}, t) = m\mathbf{v}_{\psi}(\mathbf{r}, t) = \nabla S_{\psi}(\mathbf{x}, t) \tag{27}$$

allowing to obtain the particle's equation of motion in a pseudo-Newtonian form

$$\frac{d\mathbf{p}_\psi}{dt} = -\nabla(V(\mathbf{x}, t) + Q_\psi(\mathbf{x}, t)). \quad (28)$$

The defining equations of the BB theory are similar to those of classical mechanics in the Hamilton-Jacobi formalism; compare in particular (24) with (6) and (27) with (7). However from a structural point of view, this analogy is superficial. The equations of classical mechanics arise from the flows in phase-space obeying the canonical equations of motion (the Hamilton equations, the principle of least action etc.), for any choice of canonical coordinates. Any distribution can be decomposed into elementary phase-space elements obeying these equations, i.e. the dynamics of the distribution depends on the elementary phase-space dynamics. In the de Broglie-Bohm theory on the other hand, the dynamics of the particle depends on the wavefunction (this is reflected in our notation with the indices labeled by  $\psi$ ). The law of motion for an *individual* particle depends on the *statistical distribution*  $R_\psi$  to which the particle belongs. As can be seen from (24) and (27), the dynamics of the particle is determined by the direction of the probability flow in configuration space, which becomes the only physical representation.

## 4.2 BB Trajectories in the Square Billiard

Although Bohmian trajectories have been computed for an incredibly wide variety of quantum systems, and despite that fact that the particle in a 1D box is one of the most widely used examples in any BB theory primer, very few works deal explicitly with the determination of BB trajectories in a square billiard. Bohm and Hiley (see Sect. 8.5 of Ref. [6]) employ the square billiard to give a general argument on the type of trajectories that can be expected from a wavefunction obtained by combining a few eigenstates of the Hamiltonian. This example was used as a blueprint by different authors who investigated several systems in the following years; it was explicitly applied to the square billiard a few years later [11]. It was noted, as expected, that the type of trajectory (regular, chaotic, localization) depended in a crucial way on how the initial wavefunction was constructed (the choice of the participating eigenstates and their relative weights). This was thought not to be very illuminating from the point of view of the quantum-classical correspondence, and a further work [12] examined the case when a localized wavepacket was taken as the initial wavefunction. Only BB trajectories for short times were computed, the conclusion being that the Bohmian particle propagates in a classical-like way, undergoing in particular the specular reflection on the walls. Here we give a more complete study of BB trajectories in the framework of the quantum-classical correspondence examined above. The calculations are made by integrating numerically the guidance equation (27). The results will be discussed in Sect. 5.

### 4.2.1 Simply Localized Initial State

We first compute the Bohmian trajectories in the case of Fig. 4—the initial wavefunction is a Gaussian centered at  $M$  that propagates for short times along the classical

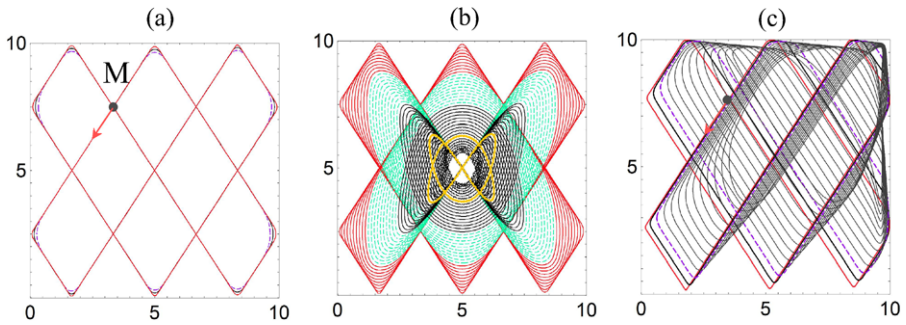


**Fig. 6** De Broglie-Bohm trajectories for a quantum state initially localized at  $M$ , whose evolution was shown in Fig. 4. (a) Short time motion when the Bohmian particle is initially localized at  $\mathbf{x}_i \equiv \mathbf{x}_M$ , the maximum of the Gaussian. The particle follows the wavepacket, leaving  $M$  in the direction of the arrow along the red trajectory until it returns at  $M$  at time  $T_{PO}$ ; the trajectory is quasi-periodic, and resembles the classical periodic orbit along which the wavepacket moves. The trajectory in the interval  $T_{PO} < t < 2T_{PO}$  is shown in black and in dashed purple for the interval  $2T_{PO} < t < 3T_{PO}$ ; actually both lines are hidden behind the previous red line except near the boundaries of the billiard, where the Bohmian particle is reflected farther away from the boundary as time increases. (b) Same as (a) for times up to  $40T_{PO}$ : the trajectory for the time interval  $0 < t < 10T_{PO}$  is shown in dark gray (red online), for  $10T_{PO} < t < 20T_{PO}$  in light dashed gray (dashed green online), and for  $20T_{PO} < t < 40T_{PO}$  in black. As  $t$  increases, the particle slows down; it still follows a periodic quasi-closed trajectory, with period  $T_{PO}$ , but within a zone restricted to the centre of the billiard slows down while restricting its motion toward the center of the billiard; the thick gray (yellow online) line represents the quasi-closed trajectory in the interval  $30T_{PO} < t < 31T_{PO}$ . (c) For the same quantum state, the trajectory for a particle with an initial position slightly off the maximum of the Gaussian ( $\mathbf{x}_i = (x_M + L/80, y_M + L/80)$ ) is shown with the same colour coding as in (a) for  $0 < t < 3T_{PO}$  and a light gray line showing the trajectory for longer times  $3T_{PO} < t < 13T_{PO}$

periodic orbit shown in Fig. 1. The BB trajectory when the initial position is chosen at  $\mathbf{x}_i \equiv \mathbf{x}_M$  (the maximum value of the distribution) is shown for short times in Fig. 6(a): the trajectory follows the wavepacket, leaving  $M$  in the direction of the arrow. The behaviour is nearly that of the classical trajectory—this is the bouncing-ball regime put in evidence in [12]—and the trajectory is quasi-periodic: the BB trajectory leaves  $M$  at  $t = 0$ , follows the line shown in red and reaches  $M$  again at the period of the classical PO  $T_{PO}$  which is also the period of the maximum of the Gaussian wavepacket. The trajectory for  $t \in [T_{PO}, 2T_{PO}]$  and  $t \in [2T_{PO}, 3T_{PO}]$  is shown in black and dashed purple respectively—it retraces the original path (in red) except near the boundaries of the billiard. There, the quantum potential gets more repulsive further from the boundaries; this is readily explained by the fact that as the Gaussian spreads, a larger portion of the Gaussian is reflected off the boundaries before the maximum of the Gaussian arrives. This creates an inversion of the net current in the direction perpendicular to the wall. As a result the Bohmian particle turns around before reaching the boundary.

The same trajectory for longer times is shown in Fig. 6(b). The colour scheme is the following: the trajectory for  $t \in [0, 10T_{PO}]$  is shown in red, for  $t \in [10T_{PO}, 20T_{PO}]$  in dashed green, and for  $t \in [20T_{PO}, 40T_{PO}]$  in black. The qualitative quasi-periodic aspect of the trajectory disappears on a longer timescale: the particle still follows an almost closed-orbit, though the shape of the orbit is progressively deformed. The ‘pseudo-period’ however does not change. It takes the same time,  $T_{PO}$ , for the particle to pass (very) near  $M$  for the first time after having been initially launched

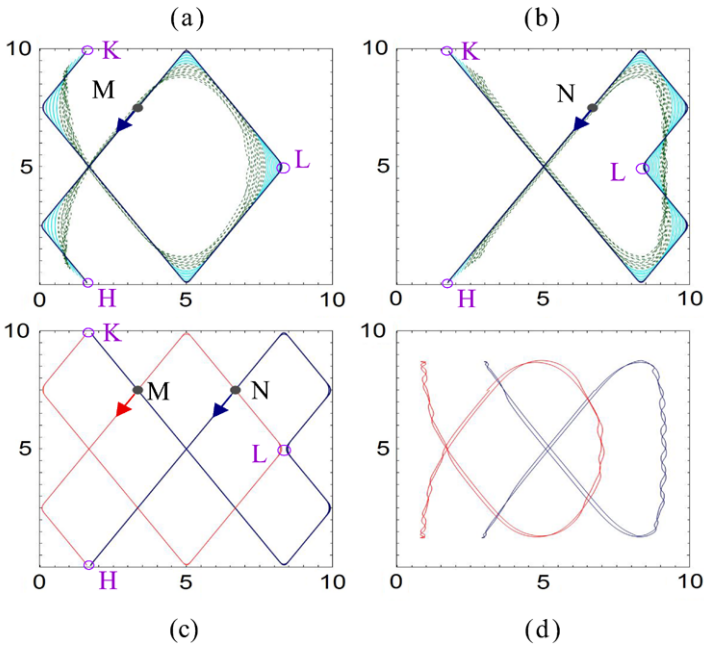
from  $M$  than to trace an almost closed orbit at longer times (see the thick yellow line in Fig. 6(b), representing the trajectory in the interval the trajectory for  $30T_{PO} < t < 31T_{PO}$ , tracing a quasi-closed orbit). The particle thus slows down, restricting its motion to a small area around the centre of the billiard.

Figure 6(c) shows the Bohmian trajectory when the initial position  $\mathbf{x}_i$  of the particle is slightly off the maximum of the Gaussian (the probability distribution there is about  $R_\psi(\mathbf{x}_i, 0)/R_\psi(\mathbf{x}_M, 0) \simeq 1/5$  of the maximum probability). For short times, the Bohmian particle follows a bouncing ball regime similar to a non-periodic classical trajectory (such as the one shown in Fig. 1(a)). However after only a few pseudo-periods, as the wavefunction spreads, the probability current drives the trajectory in the right upper quadrant of the billiard, as the particle considerably slows down.

#### 4.2.2 Doubly Localized Initial State

We now compute the Bohmian trajectories corresponding to the case portrayed in Fig. 5: the initial wavefunction is given by (22), with the probability distribution being initially concentrated in the Gaussian peaks localized at  $M$  and  $N$ . Hence in this state, the Bohmian particle is localized initially either near  $M$  or  $N$ . In a given realization one of the two wavepackets is an empty wave—it does not carry the particle but nevertheless has dynamical effects. Figure 7(a) shows the BB trajectory for a particle initially sitting at the maximum of the distribution  $\mathbf{x}_i \equiv \mathbf{x}_M$ . The trajectory for the time interval  $0 < t < T_{PO}$  is shown in dark blue in Fig. 7(a); it is also plotted in red in Fig. 7(c). The trajectory leaves  $M$  in the direction of the arrow, arrives in the zone labeled  $H$  in Fig. 7(b) with vanishing velocity; the particle then turns around, retracing almost exactly its previous path, going back through  $M$ , until it reaches the zone labeled  $K$  (without crossing the region  $L$ ); the particle turns around with vanishing velocity at  $K$  and retraces almost its previous path until it reaches  $M$  again at  $t \simeq T_{PO}$ . The particle then leaves again the  $M$  region in the direction of  $H$ ; this quasi-periodic motion is shown in Fig. 1(a) in light blue for  $T_{PO} < t < 5T_{PO}$  and in dashed green for  $5T_{PO} < t < 10T_{PO}$ . As  $t$  increases, the trajectory turns back with increasing distance from the regions around  $H$ ,  $L$  and  $K$ , and the mean velocity decreases.

Figure 7(b) shows the BB trajectory for a particle initially sitting at the maximum of the distribution  $\mathbf{x}_i \equiv \mathbf{x}_N$ , with the same colour scheme employed in Fig. 7(a). The deformation of the quasi-periodic trajectory as  $t$  increases is identical to the one seen in Fig. 7(a), except that the particle occupies a different area of the square billiard. The trajectory for  $0 < t < T_{PO}$  is also shown in dark blue (dark grey) in Fig. 7(c): the particle initially leaves  $N$  in the direction of the arrow, turns back in the  $H$  region, going back through  $N$  until it reaches  $K$  (without crossing the  $L$  region), at which point it turns back and reaches  $N$  again at  $t \simeq T_{PO}$ . Note that *taken together*, the two trajectories for Bohmian particles initially placed at  $M$  and  $N$  trace, in the interval  $0 < t < T_{PO}$ , the shape of the classical periodic orbit going through  $M$  and  $N$  (compare Fig. 7(c) with Figs. 6(a) and 1(a)). This is to be expected, since for short times, the distribution does not spread significantly and each wavepacket initially centered at  $M$  and  $N$  moves by following the periodic orbit. Of course this is not



**Fig. 7** De Broglie-Bohm trajectories for the quantum state given by (22), initially localized at  $M$  and  $N$  whose evolution was shown in Fig. 5. (a) Trajectory obtained when the Bohmian particle is initially localized at  $\mathbf{x}_i \equiv \mathbf{x}_M$ . The particle leaves with the wavepacket in the direction of arrow, turns around at  $H$ , then  $K$ , and arrives at  $M$  in a time  $T_{PO}$  (dark line, dark blue online). The motion in the time intervals  $T_{PO} < t < 5T_{PO}$  and  $5T_{PO} < t < 10T_{PO}$  is shown in light gray (light blue online) and dashed dark gray (dashed green online) respectively. (b) Same as (a) but when the Bohmian particle is initially localized at  $\mathbf{x}_i \equiv \mathbf{x}_N$ . (c) Bohmian trajectories for  $0 < t < T_{PO}$  taken from (a) and (b) plotted together; the overall shape is very similar to that of the classical periodic orbit of Fig. 1 going through  $M$  and  $N$ . (d) Same as (c) for  $10T_{PO} < t < 11T_{PO}$

the case for longer times: Fig. 7(d) shows the same Bohmian trajectories initially launched from  $N$  and  $N$  for times  $10T_{PO} < t < 11T_{PO}$  (compare with Fig. 6(b)).

The main feature visible for the BB trajectories in the doubly localized initial state is the reflection that the particle undergoes at  $H$ ,  $L$  and  $K$ . This behaviour has no classical counterpart: it is the result of the interference of the two Gaussian amplitudes at these points. Indeed the center of the two Gaussians cross at these points; Fig. 5(c) illustrates the case of a constructive interference at  $L$ . Here the two wavepackets have opposite components along the  $x$  axis, so the net probability density current along  $x$  decreases as the two Gaussians start to interfere. The particle, moving before the crossing point along with the localized wavepacket, slows down, whereas the Gaussians keep moving with constant group velocity. Ultimately the net current in the  $x$  direction reverses before the particle reaches the crossing point, thereby giving rise to the avoided crossing type of behaviour at  $L$  (for a general detailed investigation of quantum trajectory behaviour when Gaussian wavepackets interfere, see [13]). When the net current is reversed in both the  $x$  and  $y$  directions, the Bohmian particle’s motion is reversed; this is what happens in the  $H$  and  $K$  regions. In this respect, it may be noted that the empty wavepacket (the Gaussian that, before the crossing, does

not carry the particle) produces the same dynamical effect than the reflection on the billiard's boundaries. Indeed, at  $H$  and  $K$  the reversal of the probability current along  $x$  is due to the empty wavepacket, whereas the reversal in the  $y$  direction is produced by the reflection of the Gaussian wavepacket on the boundary walls.

## 5 Discussion

### 5.1 The Quantum-Classical Correspondence

The term ‘quantum-classical correspondence’, as employed in this paper, reflects the use that is usually made in works undertaken in the field of ‘quantum chaos’. It is indeed well-known that when the classical action appearing in the path integral expression for the propagator  $K(\mathbf{x}_0, \mathbf{x}, t)$  is much larger than  $\hbar$ , then  $K(\mathbf{x}_0, \mathbf{x}, t)$  can be approximately written in terms of the sole classical paths relating  $\mathbf{x}_0$  to  $\mathbf{x}$ . This allows to understand the properties of quantum systems (such as the distribution of the energy levels, scars in the wavefunctions, recurrences in the time-dependent behaviour of the system) in terms of the properties of the analog classical system [16, 17]. Such a correspondence is particularly useful in the studies of nonseparable quantum systems, for which quantum computations are either nonfeasible or yield uninterpretable results.

In the square billiard, the quantum-classical correspondence is extremely simple: the semiclassical form of the propagator (16) is exact meaning that each point of the quantum wavefunction propagates along a classical trajectory. This explains the correspondence between the dynamics of the classical distributions (Figs. 2 and 3) and those of the quantum distributions (Figs. 4 and 5). The dynamical evolution in the classical and quantum cases is essentially identical, the important difference being of course that classically the probability *distribution* evolves by following the classical trajectories, whereas quantum mechanically the *wavefunction* evolves by following the classical trajectories, the distribution resulting from the interference of different bits of the wavefunction each carried by a classical trajectory.

Hence the quantum-classical correspondence is only dynamical—it remains silent on the ontological aspects. The classical ensemble is a statistical distribution of point-like particles in phase-space, giving the probability distribution in configuration space as a function of time for a fixed initial distribution. The quantum ensemble appears as the intensity of a field (here presented in configuration space). Although the field moves by following the classical motion, it cannot be associated with a distribution of point-like particles—the field interferes and only its intensity represents the statistical distribution.

### 5.2 Properties of Bohmian Trajectories

From (24) and (27), it is straightforward to establish [1] that the de Broglie-Bohm trajectories follow the streamlines of the probability flow, the velocity of the Bohmian particle depending on the local current density  $\mathbf{j}_\psi$  through

$$\mathbf{j}_\psi(\mathbf{x}, t) = R_\psi(\mathbf{x}, t)\mathbf{v}_\psi(\mathbf{x}, t). \quad (29)$$

Hence if the wavefunction is a localized wavepacket, the particle will be restricted to move with the wavepacket; in a coarse-grained sense, the particle's motion follows that of the wavepacket, irrespective of its precise initial position. This is particularly clear in Fig. 6(a): the wavepacket initially sharply localized at  $M$  follows the classical periodic orbit of Fig. 1(a). The BB trajectory therefore also follows the classical trajectory, except near the boundary of the billiard where the part of the wavepacket that is traveling ahead of the Bohmian particle's position is reflected, thereby reversing the current density and preventing the particle from reaching the boundary.

As the wavepacket spreads over substantial portions of the billiard, each Bohmian trajectory will be sensitive to very fine details of the probability flow, implying a crucial dependence of the trajectory on the initial distribution and the initial position. In Fig. 6(b), when the initial position lies on the top of the Gaussian, the ensuing trajectory is symmetric around the center of the billiard, whereas when the initial position is slightly off the center of the Gaussian (Fig. 6(c)) the fixed point is in the upper right-hand corner. Given that locally the probability flows have no relation to the classical dynamics of the billiard, the BB trajectories will be unrelated to the classical ones.

The example portrayed in Fig. 7, corresponding to a doubly localized initial state, shows that even for short times and localized wavepackets, BB trajectories can be markedly different from the classical ones. This is well illustrated in Fig. 7(c): although each of the localized wavepackets launched from  $M$  and  $N$  follows the classical periodic orbit of Fig. 1(a), when these wavepackets cross the net current density can locally vanish and reverse its course. This is why taken together, the two Bohmian trajectories are able to recover the periodic orbit. This is to be expected, since on a statistical basis BM matches the quantum mechanical predictions showing wavepacket propagation along the classical orbit. Notwithstanding if the dynamics predicted by the de Broglie-Bohm theory is taken as a realist account of quantum phenomena, an individual particle follows “in reality”<sup>1</sup> one of the two non-classical Bohmian trajectories (depending on its initial position), the classical orbit appearing as a statistical artifact.

### 5.3 Bohmian Mechanics and the Classical Limit

It is well-known that typical Bohmian trajectories are not classical. As such, this feature is not necessarily a problem, provided one can account unambiguously for the emergence of classical mechanics. However achieving the classical limit turns out to be an intricate problem (see Chap. 6 of [1]). It is generally admitted [6, 18–22] that BB trajectories in closed systems being generically non-classical, in order to emerge, classical mechanics calls for a special class of states combined with environmental

---

<sup>1</sup>The main experimental realization of 2D quantum billiards consist of mesoscopic devices such as quantum dots [14], containing an electron in a cavity having a definite shape; the properties of the electron such as the conductance peaks, are correlated with the periodic orbits of the corresponding classical cavity. It is still difficult to control precisely the wavefunction in a quantum dot so as to create a doubly localized Gaussian state. However doubly-localized states are routinely created by tailored laser excitation of the outer electron in Rydberg atoms [15].

interactions. More precisely, following an initial suggestion made by Bohm and Hiley [6], it has been argued [19–21] that Bohmian mechanics in the classical limit must involve a mechanism yielding a localized and non-spreading packet behaving quasi-classically. This mechanism can only arise when the closed system interacts with an environment inducing decoherence.

Relying on decoherence to recover classical trajectories from non-classical ones raises a number of problems. First, as we have discussed elsewhere [23], this argument appears as somewhat specious when applied to semiclassical systems: in closed semiclassical quantum systems, the wavefunction as well as several observable properties already display the fingerprints of the underlying classical dynamics. The Bohmian particle has a non-classical motion, but this motion is determined by a wavefunction that is itself built from the underlying classical structure and displays classical morphological features. In this respect, the square billiard is a simple semiclassical system, for which, as shown above, the quantum-classical correspondence is straightforward; several quantities not discussed in the present work (like recurrences in the autocorrelation function) can also be given a semiclassical explanation in terms of the large-scale structures determined by the underlying classical dynamics. As already mentioned (see also [24, 25]), the de Broglie-Bohm account of such features involves non-classical trajectories following the streamlines of the flow. Only globally are the classical structures recovered on a statistical basis, like the classical periodic orbit obtained in Fig. 7(c) by combining two individual non-classical Bohmian trajectories.

Second, decoherence actually involves averaging over the “measurements” performed by the environment. Relying on this effect to achieve classicality faces well-known interpretational problems [26]. Indeed, the reduced density matrix becomes diagonal for all practical purposes, but the total wavefunction remains entangled, and it is only by reinterpreting the reduced density matrix that a pure state is transformed into an improper [27] statistical mixture. From a de Broglie-Bohm dynamics point of view, the total wavefunction has several branches corresponding to the simultaneous couplings with the environmental states. Each interaction of the system with the environment leads to only one branch of the wavefunction being active (the one containing the particle); the other branches are the so-called “empty waves”—they still exist and can potentially become active (and interfere) again, unless they are suppressed by hand, in an ad-hoc manner (this is done for example when discussing measurements in Sect. 8.3. of [1]). In the absence of a dynamical theory for the empty waves (maybe supplemented by an account of the observation process in which only the particle would give rise to a psychophysical parallelism, see Ref. [28]), the collapse is only apparent and the emergence of classical dynamics is not ensured.

The third point concerns the specific conditions under which decoherence will turn Bohmian into classical trajectories. As a general rule decoherence converts, for practical purposes, a pure state into a mixed state without necessarily implying non-spreading probability distributions. There is no universal dynamical mechanism that will achieve this, but the tentative models given in [6, 19–21] all rely on obtaining non-spreading wave-packets behaving quasi-classically. Note however that demanding the classical limit to be achieved by non-spreading mixtures does not require any of the specific resources of the de Broglie-Bohm theory—any other interpretation

of quantum phenomena that can dispose of (or rather, accept) the interpretational problems associated with the post-decoherence improper mixtures is as effective as Bohmian mechanics in achieving classical motion. Indeed, if decoherence is taken as being successful in recovering classicality, by phenomenologically associating a classical particle with a localized non-spreading wavepacket moving on classical trajectories, there is no need to postulate the existence of a point-like particle pursuing well-defined trajectories. The specific epistemological assets of the de Broglie-Bohm interpretation would then play no role in accounting for the emergence of classicality.

Finally, in line with the first remark it can be objected [29, 30] whether requiring localized and non-spreading mixtures is the proper way to achieve the classical limit. Classically, the spreading is the result of the Liouville diffusion of the statistical distribution. Since the quantum-mechanical statistical distribution depends on the wavefunction, there is no fundamental reason to constrain the wavefunction to avoid spreading. The problem for Bohmian particle dynamics is that the spreading necessarily brings in interferences (e.g. when the wavepacket hits the billiard's boundary), making it impossible to recover classical motion if the particle moves along a given streamline of the flow. This conclusion was already put forward in different terms by Holland [18] who noted that neither pure nor mixed states allowed to generate classical motion from the ensuing probability flow.

## 6 Conclusion

In this work, we have investigated Bohmian trajectories in a square billiard and contrasted them with quantum wavepacket dynamics and with the trajectories of the classical square billiard. As expected from a path integral approach, the quantum square billiard displays dynamics abiding by the quantum-classical correspondence—each bit of the spreading quantum wavefunction propagates along a classical trajectory. On the other hand, individual Bohmian trajectories were shown to be generically highly non-classical, although statistically the underlying classical large scale structures are recovered as expected. We have also argued that the inclusion of decoherence is unlikely to allow de Broglie-Bohm dynamics to recover classicality. This conflict between the dynamical continuity involving the classical propagation of the wavefunction and the persistence of non-classical, typically quantum features of the probability distribution on smaller scales is not limited to the de Broglie-Bohm interpretation—it is relevant to the study of the quantum-classical transition irrespective of any particular interpretation. However, this conflict does take an acute form for Bohmian mechanics because the ontological claims made by this interpretation involve a continuity with the ontology of classical mechanics.

## References

1. Holland, P.R.: *The Quantum Theory of Motion*. Cambridge University Press, Cambridge (1993)
2. Cushing, J.T.: The causal quantum theory program. In: Cushing, J.T., Fine, A., Goldstein, S. (eds.) *Bohmian Mechanics and Quantum Theory: An Appraisal*. Boston Studies in the Philosophy of Science, vol. 184, pp. 1–19. Kluwer, Dordrecht (1996)

3. Bohm, D., Hiley, B.J.: Unbroken quantum realism from microscopic to macroscopic levels. *Phys. Rev. Lett.* **55**, 2511–2514 (1985)
4. Home, D.: *Conceptual Foundations of Quantum Physics: An Overview from Modern Perspectives*. Plenum, London (1997)
5. Einstein, A.: Elementare Überlegungen zur Interpretation der Grundlagen der Quanten-Mechanik. In: *Scientific Papers Presented to Max Born*, pp. 33–40. Hafner, New York (1953)
6. Bohm, D., Hiley, B.J.: *The Undivided Universe: An Ontological Interpretation of Quantum Theory*. Routledge, London (1993)
7. Doncheski, M.A., Heppelmann, S., Robinett, R.W., Tussey, D.C.: Wave packet construction in two-dimensional quantum billiards: Blueprints for the square, equilateral triangle, and circular cases. *Am. J. Phys.* **71**, 541 (2003)
8. Goldstein, H.: *Classical Mechanics*. Addison-Wesley, Reading (1980)
9. Kleinert, H.: *Path Integrals in Quantum Mechanics, Statistics, Polymer Physics, and Financial Markets*. World Scientific, Singapore (2006)
10. Schulman, L.S.: *Techniques and Applications of Path Integration*. Wiley, New York (1981)
11. Alcantara-Bonfim, O.F., de Florencio, J., Sa Barreto, F.C.: Chaotic dynamics in billiards using Bohm's quantum dynamics. *Phys. Rev. E* **58**, R2693–R2696 (1998)
12. de Sales, X., Florencio, J.: Bohmian quantum trajectories in a square billiard in the bouncing ball regime. *Physica A* **290**, 101–106 (2001)
13. Sanz, A.S., Miret-Artes, S.: A trajectory-based understanding of quantum interference. *J. Phys. A, Math. Theor.* **41**, 435303 (2008)
14. Alhassid, Y.: The statistical theory of quantum dots. *Rev. Mod. Phys.* **70**, 895–968 (2000)
15. Noordam, L.D., Jones, R.R.: Probing Rydberg electron dynamics. *J. Mod. Opt.* **44**, 2515–2532 (1997)
16. Haake, F.: *Quantum Signatures of Chaos*. Springer, Berlin (2001)
17. Gutzwiller, M.C.: *Chaos in Classical and Quantum Mechanics*. Springer, Berlin (1990)
18. Holland, P.R.: Is quantum mechanics universal. In: Cushing, J.T., Fine, A., Goldstein, S. (eds.) *Bohmian Mechanics and Quantum Theory: An Appraisal*. Boston Studies in the Philosophy of Science, vol. 184, pp. 99–110. Kluwer, Dordrecht (1996)
19. Appleby, D.M.: Generic Bohmian trajectories of an isolated particle. *Found. Phys.* **29**, 1863–1883 (1999)
20. Appleby, D.M.: Bohmian trajectories post-decoherence. *Found. Phys.* **29**, 1885–1916 (1999)
21. Bowman, G.: On the classical limit in Bohm's theory. *Found. Phys.* **35**, 605–625 (2005)
22. Ban, B.L.: Violation of the correspondence principle: breakdown of the Bohm-Newton trajectory correspondence in a macroscopic system. *Phys. Rev. A* **61**, 032105 (2000)
23. Matzkin, A., Nurock, V.: Classical and Bohmian trajectories in semiclassical systems: Mismatch in dynamics, mismatch in reality? *Stud. Hist. Philos. Sci. B* **39**, 17–40 (2008)
24. Matzkin, A.: Rydberg wavepackets in terms of hidden-variables: de Broglie-Bohm trajectories. *Phys. Lett. A* **345**, 31–37 (2005)
25. Matzkin, A.: Can Bohmian trajectories account for quantum recurrences having classical periodicities? *Phys. Lett. A* **361**, 294–300 (2007)
26. Leggett, A.: Testing the limits of quantum mechanics: motivation, state of play, prospects. *J. Phys., Condens. Matter* **14**, R415–R451 (2002)
27. d'Espagnat, B.: *Conceptual Foundations of Quantum Mechanics*. Westview Press, Reading (1999)
28. Zeh, H.D.: Measurement in Bohm's versus Everett's quantum theory. *Found. Phys.* **18**, 723–730 (1988)
29. Wiebe, N., Ballentine, L.E.: Quantum mechanics of Hyperion. *Phys. Rev. A* **72**, 022109 (2005)
30. Ballentine, L.E.: Classicality without decoherence. *Found. Phys.* **38**, 916–922 (2008)